DALTON
FULL PAPER

Synthesis, structure and kinetics of Group 6 metal carbonyl complexes containing a new 'P_2N' mixed donor multidentate ligand †

Eric W. Ainscough,* Andrew M. Brodie,* Paul D. Buckley, Anthony K. Burrell, Steven M. F. Kennedy and Joyce M. Waters

Chemistry - Institute of Fundamental Sciences, Massey University, Private Bag 11-222, Palmerston North, New Zealand. E-mail: A.Brodie@massey.ac.nz

Received 28th March 2000, Accepted 20th June 2000
Published on the Web 27th July 2000

The 'P_2N' mixed donor ligand 2-(diphenylphosphino)-*N*-[2-(diphenylphosphino)benzylidene]aniline (PNCHP) reacted with $[Cr(CO)_4(NBD)]$ and $[M(CO)_4(C_5H_{11}N)_2]$ (M = Mo or W; NBD = norbornadiene; $C_5H_{11}N$ = piperidine) to yield *cis*-$[Cr(CO)_4(PNCHP\text{-}\kappa^2N,P)]$ and *cis*-$[M(CO)_4(PNCHP\text{-}\kappa^2P,P')]$ respectively. PNCHP behaves as a 'P,N' bidentate ligand when M is Cr and a 'P,P' bidentate ligand when M is Mo or W. Heating *cis*-$[Cr(CO)_4(PNCHP\text{-}\kappa^2N,P)]$ or *cis*-$[M(CO)_4(PNCHP\text{-}\kappa^2P,P')]$ (M = Mo or W) in toluene affords the complexes *mer*-$[M(CO)_3(PNCHP\text{-}\kappa^3P,N,P')]$ (M = Cr, Mo or W). Reaction of PNCHP with $[Mo(CO)_3(CHT)]$ (CHT = 1,3,5-cycloheptatriene) in cold toluene yields *fac*-$[Mo(CO)_3(PNCHP\text{-}\kappa^3P,N,P')]$ which readily isomerises to *mer*-$[Mo(CO)_3(PNCHP\text{-}\kappa^3P,N,P')]$ in solution. PNCHP reacts with UV-irradiated tetrahydrofuran solutions of $[M(CO)_6]$ (M = Cr or W) to yield phosphorus bound co-ordination isomers of $[M(CO)_5(PNCHP\text{-}\kappa^1P)]$. The same reaction when carried out with one half equivalent of PNCHP yields the PNCHP bridged dinuclear species $[\{M(CO)_5\}_2(PNCHP\text{-}\kappa^2P,P')]$. The compounds have been characterised by spectroscopic means and the single crystal structures of *cis*-$[Cr(CO)_4(PNCHP\text{-}\kappa^2N,P)]$, *cis*-$[W(CO)_4(PNCHP\text{-}\kappa^2P,P')]$, *mer*-$[Mo(CO)_3(PNCHP\text{-}\kappa^3P,N,P')]$ and $[\{W(CO)_5\}_2(PNCHP\text{-}\kappa^2P,P')]$ determined. In addition, the isomerisation kinetics of *fac*- to *mer*-$[Mo(CO)_3(PNCHP\text{-}\kappa^3P,N,P')]$ has been studied to determine rate constants and thermodynamic activation parameters.

The mixed donor ligand, 2-(diphenylphosphino)-*N*-[2-(diphenylphosphino)benzylidene]aniline (PNCHP), can be visualised as two triphenylphosphine moieties tethered together in the *ortho* positions by an imine linker. Since the imine bond has no plane of symmetry perpendicular to the C=N axis, the two phosphorus atoms are inequivalent which provides an excellent handle for characterising the metal complexes in solution by ^{31}P NMR.

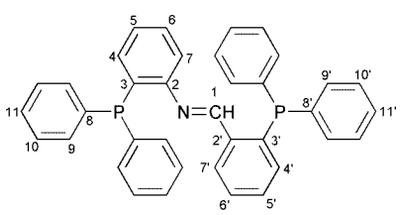

PNCHP

In this study we set out to establish the co-ordination preferences of the potentially tridentate 'P_2N' ligand in an octahedral environment. The Group 6 metal carbonyls were chosen because they offer an entry point into the realms of organometallic chemistry where such mixed donor ligand types have shown promise in catalysis.[1] One set of results obtained enabled the *fac*-to-*mer* isomerisation of the complex $[Mo(CO)_3(PNCHP)]$ to be characterised *via* a kinetic study. Recently, *fac–mer* isomerisation involving a tridentate 'P_2N' mixed donor ligand has been implicated in the C–C bond cleavage of terminal alkynes by water.[2] Kleverlaan *et al.* give a concise background to *fac–mer* isomerisation[3] and in general the unassisted *fac–mer* isomerisation in six-co-ordinate octahedral complexes can occur in either of two ways. First, dissociation of a ligand can be followed by rearrangement of the resultant five-co-ordinate co-ordinatively unsaturated intermediate.[4] Secondly, rearrangement may occur *via* a non-dissociative intramolecular mechanism.[5] The majority of kinetic studies put forward to support either of the above isomerisation mechanisms have involved ligands of the mono- and/or bi-dentate variety.[3,6,7] To our knowledge only one kinetic study has been reported involving a tridentate ligand.[8]

† Electronic supplementary information (ESI) available: NMR data for the ligand, analytical and mass spectral data for the complexes. See http://www.rsc.org/suppdata/dt/b0/b002427i/

Results and discussion

Synthesis and characterisation of PNCHP

The Schiff base condensation reaction of 2-diphenylphosphinobenzenaldehyde with 2-aminophenyldiphenylphosphine in refluxing benzene yields the 'P_2N' ligand PNCHP. The choice of solvent is important since this reaction does not proceed in refluxing ethanol. PNCHP possesses two inequivalent phosphorus atoms and this is supported by the appearance of two signals at δ −14.2 and −14.8 [with no observable J(P–P) coupling] in the $^{31}P\text{-}\{^1H\}$ NMR spectrum. The $^{13}C\text{-}\{^1H\}$ and ^1H NMR spectral data, with assignments made using standard 2-D correlation and attached proton test (APT) techniques, are available as supplementary data. The proton spectrum displays an imine proton resonance at δ 8.92 which is split into a doublet by the nearest phosphorus atom with a coupling constant of 5.5 Hz [^4J(PH)]. Four of the aromatic protons (H^4, H^5, H^7, $H^{5'}$ and $H^{7'}$) which are attached to the two central rings can clearly be identified at δ 7.03, 6.74, 7.96, 6.81 and 6.46 since they fall outside the main aromatic multiplet δ (7.16–7.36). In the $^{13}C\text{-}\{^1H\}$ spectrum the imine carbon (C^1) signal is the highest frequency resonance, appearing as a doublet at δ 157.9 [^3J(PC) 25.0 Hz].

DOI: 10.1039/b002427i

Table 1 ^{31}P-{^{1}H} NMR [a] and proton NMR [b] data

Complex	^{31}P-{^{1}H} NMR			^{1}H NMR	
	δ	^{2}J(PMP)/Hz	^{1}J(MP)/Hz	δ(N=CH)	^{4}J(PH)/Hz
1 *mer*-[Cr(CO)$_3$(PNCHP)]	79.6, 74.7	[c]		8.28 (s)	
2 *mer*-[Mo(CO)$_3$(PNCHP)]	59.0 (d), 53.7 (d)	93		8.56 (s)	
3 *mer*-[W(CO)$_3$(PNCHP)]	45.0 (d), 36.6 (d)	88	313, 315	8.50 (s)	
4 *fac*-[Mo(CO)$_3$(PNCHP)]	39.4 (d), 36.3 (d)	26		8.87 (s)	
5 *cis*-[Cr(CO)$_4$(PNCHP)]	53.2 (s), −19.0 (s)			[c]	
6 *cis*-[Mo(CO)$_4$(PNCHP)]	36.9 (d), 19.8 (d)	26		8.06 (s)	
7 *cis*-[W(CO)$_4$(PNCHP)]	22.2 (d), 3.0 (d)	27	238, 233	8.13 (s)	
8 [{Cr(CO)$_5$}$_2$(PNCHP)]	55.2 (s), 54.2 (s)			8.65 (s)	
9 [{W(CO)$_5$}$_2$(PNCHP)]	19.2 (s), 18.1 (s)		244, 243	8.73 (s)	
10a [Cr(CO)$_5$(PNCHP)]	54.1 (s), −14.6 (s)			9.13 (d)	6.2
10b [Cr(CO)$_5$(PCHNP)]	54.5 (s), −15.6 (s)			8.44 (s)	
11a [W(CO)$_5$(PNCHP)]	18.6 (s), −15.6 (s)		244	9.13 (d)	6.1
11b [W(CO)$_5$(PCHNP)]	18.1 (s), −14.8 (s)		242	8.52 (s)	

[a] Recorded at 109 MHz, chemical shifts are in ppm relative to 85% H_3PO_4, solvent $CDCl_3$. [b] Recorded at 270 MHz, chemical shifts are in ppm relative to TMS, solvent $CDCl_3$. [c] Not resolved.

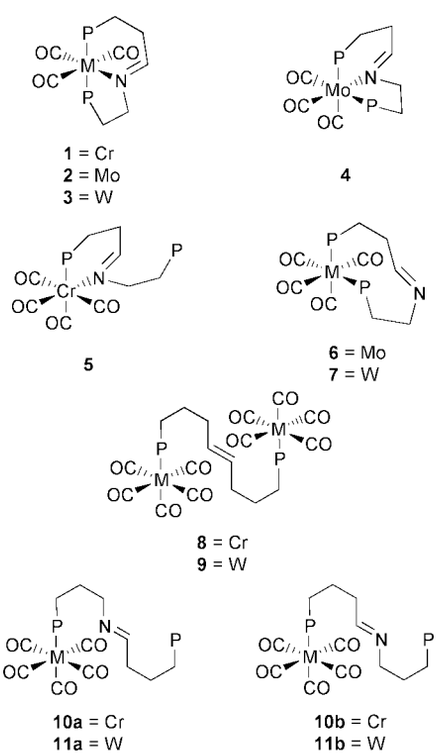

Fig. 1 The complexes showing the various co-ordination modes of PNCHP with the phenyl rings omitted for clarity.

Synthesis of PNCHP complexes

The complexes [M(CO)$_x$(PNCHP)] (x = 3, 4 or 5, M = Cr, Mo or W) and [{M(CO)$_5$}$_2$(PNCHP)] (M = Cr or W) were prepared by conventional methods as described in the Experimental section. The air stable complexes all eventually convert in solution at room temperatures to *mer*-[M(CO)$_3$(PNCHP-κ^3*P*,*N*,*P*′)], depicted by **1**, **2** and **3** in Fig. 1, with the exception of the pentacarbonyl dimer species. This process takes hours for *fac*-[Mo(CO)$_3$(PNCHP-κ^3*P*,*N*,*P*′)] **4**, days for *cis*-[Mo(CO)$_4$(PNCHP-κ^2*P*,*P*′)] **6** and months for [Cr(CO)$_5$(PNCHP-κ^1*P*)] **10a** and **10b**. The reverse reactions were not observed when dichloromethane solutions of the *mer* complexes were exposed to carbon monoxide gas at standard atmospheric pressure. The lability of similar systems, with respect to stability towards air and carbon monoxide substitution, appears to depend on the ease with which the nitrogen donor can be displaced. For example, in contrast to the tricarbonyl complexes in this paper, the 'P$_2$N' complex *fac*-[Mo(CO)$_3${CH$_3$C(CH$_2$NHCH$_3$)(CH$_2$PPh$_2$)$_2$-κ^3*P*,*N*,*P*′}] decomposes in air, even in the solid state, and reacts spontaneously with carbon monoxide at standard atmospheric pressure to give the 'P,P' complex *cis*-[Mo(CO)$_4${CH$_3$C(CH$_2$NHCH$_3$)(CH$_2$PPh$_2$)$_2$-κ^2*P*,*P*′}].[9] The complexes are labelled and depicted in Fig. 1, NMR data are listed in Table 1, infrared and electronic spectral data in Table 2 and mass spectral (LSIMS) and microanalytical results, which are consistent with the formulations, have been deposited.

The key to obtaining the kinetic product *fac*-[Mo(CO)$_3$(PNCHP-κ^3*P*,*N*,*P*′)] **4** was its low solubility in toluene below 20 °C, enabling it to precipitate before its conversion into the thermodynamically favoured *mer* isomer. This facile conversion is most likely due to the ability of PNCHP easily to adopt the stable planar configuration when in the *mer* form. Unfortunately, the corresponding *fac* chromium and tungsten analogues could not be prepared, hence the *fac*-to-*mer* isomerisation kinetics was only carried out for the molybdenum complex. Kinetic and thermodynamic data for this isomerisation are shown in Table 3.

Single crystal X-ray diffraction studies

Crystal structure of *mer*-[Mo(CO)$_3$(PNCHP-κ^3*P*,*N*,*P*′)]·2C$_6$H$_5$Me 2. In complex **2** (Fig. 2 and Table 4), which has a *trans* arrangement of phosphorus atoms, the P(1)–Mo–P(2) angle is constrained from the ideal octahedral angle of 180° to be 159.29(3)° as a result of the strain imposed by the 5-membered chelate ring. This angle is typical of molybdenum carbonyl complexes containing five-membered chelate rings.[11,12] As expected the carbonyl ligand which is *trans* to the N atom (Mo–C(3)) has a shorter Mo–C distance of 1.954(3) Å than the two carbonyl groups which are *trans* to one another (Mo–C(2), 2.019(3); Mo–C(4), 2.014(3) Å). The C(12)–N, N–C(1) and C(1)–C(42) bond lengths of 1.486(4), 1.258(3) and 1.445(4) Å respectively show that there is little, if any, electron delocalisation through the imine system. These lengths are similar to accepted values for C–N, C=N, and C–C bonds which are *exo* to an aromatic ring.[13] (Similar results are found for **7**, **5** and **9**.) The Mo–N distance of 2.237(2) Å is similar to the lengths (2.294(3) and 2.278(4) Å) previously found in *cis*-[Mo(CO)$_4${(CH$_3$)(C$_6$H$_5$)C=N(CH$_2$)}$_2$-κ^2*N*,*N*′)].[12] The Mo–P distances of 2.425(2) and 2.431(2) Å do not differ significantly from one another despite the chemical inequivalence of the two P atoms. Similarly the six P–C bond lengths, which lie in the range 1.834(3)–1.840(3) Å, are in close agreement to each other.

Crystal structure of *cis*-[W(CO)$_4$(PNCHP-κ^2*P*,*P*′)]·0.5CHCl$_3$ 7. In complex **7** (Fig. 3 and Table 5), where the two P atoms occupy *cis* co-ordination sites, the largest deviation from the ideal co-ordination geometry is found, not unexpectedly, with the P(1)–W–P(2) angle of 102.27(4)° (*cf.* P(1)–Mo–P(2) of

Table 2 Infrared and electronic absorption data

Complex	IR/cm^{-1} ν(C≡O)[a]	ν(C=N)[b]	UV-vis λ/nm (ε_{max}/L mol^{-1}cm^{-1})[c]
1	1944w, 1847vs, 1828 (sh)	[d]	628 (1800)
2	1956w, 1857vs, 1836 (sh)	[d]	574 (1900) 551 (2200)[e] 586 (sh) (2500)[f]
3	1948w, 1846vs, 1824 (sh)	1571w	580
4	1932s, 1843s, 1825s[b]	1586w	536
5	2001m, 1911s, 1893s, 1857m	1582m	396 (2700)
6	2019m, 1919vs, 1900vs, 1865m	1634w	
7	2014m, 1911vs, 1892vs, 1863m	1637w	
8	2063m, 1983w, 1940s	1618w	
9	2071m, 1981w, 1938s	1613w	
10a,**10b**[g]	2063m, 1984w, 1940s	1614w	
11a,**11b**[g]	2071m, 1982w, 1939s	[d]	

[a] In $CHCl_3$. [b] As Nujol mull. [c] M ⟶ π^*_{imine} charge transfer band in $CHCl_3$. [d] Not assigned. [e] In acetone. [f] In toluene. [g] Isomer mixture.

Table 3 First-order rate constants and activation energies[a] for geometrical isomerisation of *fac*-to-*mer*-[Mo(CO)$_3$(PNCHP-κ*P*,*N*,*P*′)]: $k_{obsd} = k_1 + k_{-1}$, $K_{eq} = k_1/k_{-1} = 7.3$

Solvent	*T*/°C	10^{-5} k_{obsd}/s^{-1}	10^{-5} k_1/s^{-1}	10^{-5} k_{-1}/s^{-1}
Acetone	19.5	1.39	1.22	0.170
	29.7	4.75	4.18	0.574
	40.0	19.6	17.2	2.08
	49.5	55.6	48.9	6.71
Acetone/Et_3N[b]	19.8	1.37	[c]	
CH_2Cl_2	19.4	3.46	[c]	
MeCN	40.0	11.6	[c]	

[a] $\Delta H_1^{\ddagger} = 95 \pm 3$ kJ mol^{-1}, $\Delta H_{-1}^{\ddagger} = 94 \pm 2$ kJ mol^{-1}, $\Delta S_1^{\ddagger} = -14.1 \pm 0.7$ J K^{-1} mol^{-1}, $\Delta S_{-1}^{\ddagger} = -36 \pm 2$ J K^{-1} mol^{-1}. [b] 2 mol equivalents of triethylamine. [c] K_{eq} not recorded.

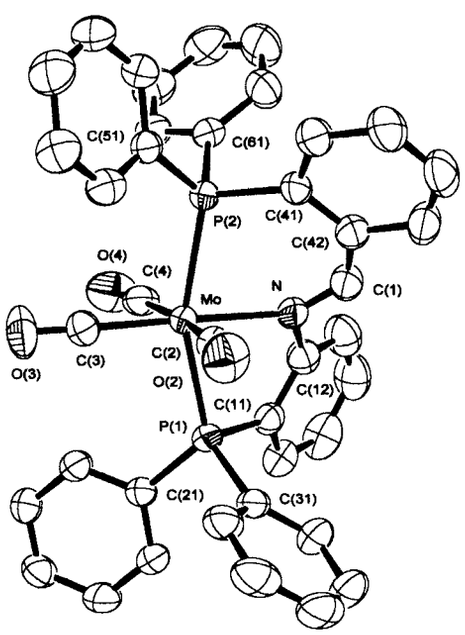

Fig. 2 An ORTEP[10] diagram for the complex *mer*-[Mo(CO)$_3$(PNCHP-κ^3*P*,*N*,*P*′)] **2** showing the numbering system used. Thermal ellipsoids are at the 50% probability level. Hydrogen atoms have been omitted for reasons of clarity.

104.62(7)° found in *cis*-[Mo(CO)$_4$(PPh$_3$)$_2$][12]). There is a small difference in the two W–P bond lengths (W–P(1), 2.5749(12); W–P(2), 2.5576(14) Å) but both are very similar to those observed in other tungsten–carbonyl containing derivatives where the triphenylphosphine is *trans* to a carbonyl group.[14] No significantly different distances in the W–C bond lengths are noted for the two carbonyl ligands in *trans* co-ordination sites

Table 4 Selected bond lengths [Å] and angles [°] for *mer*-[Mo(CO)$_3$(PNCHP-κ^3*P*,*N*,*P*′)]·2C$_6$H$_5$Me

Mo–P(1)	2.431(2)	P(2)–C(41)	1.840(3)
Mo–P(2)	2.425(2)	P(2)–C(51)	1.838(3)
Mo–N	2.237(2)	P(2)–C(61)	1.836(3)
Mo–C(2)	2.019(3)	O(2)–C(2)	1.148(3)
Mo–C(3)	1.954(3)	O(3)–C(3)	1.162(3)
Mo–C(4)	2.014(3)	O(4)–C(4)	1.152(3)
P(1)–C(11)	1.834(3)	N–C(1)	1.258(3)
P(1)–C(21)	1.836(3)	N–C(12)	1.486(4)
P(1)–C(31)	1.840(3)	C(1)–C(42)	1.445(4)
P(2)–Mo–P(1)	159.29(3)	C(51)–P(2)–Mo	119.74(9)
C(2)–Mo–P(1)	91.92(8)	C(61)–P(2)–Mo	120.49(9)
C(3)–Mo–P(1)	101.33(8)	O(2)–C(2)–Mo	175.4(2)
C(4)–Mo–P(1)	89.11(8)	O(3)–C(3)–Mo	177.8(2)
C(2)–Mo–P(2)	86.79(8)	O(4)–C(4)–Mo	173.3(3)
C(3)–Mo–P(2)	99.27(8)	C(1)–N–Mo	129.8(2)
C(4)–Mo–P(2)	95.36(8)	C(12)–N–Mo	114.3(2)
N–Mo–P(1)	76.71(6)	C(11)–P(1)–C(21)	105.79(11)
N–Mo–P(2)	82.82(6)	C(11)–P(1)–C(31)	103.60(12)
C(2)–Mo–C(3)	87.66(11)	C(21)–P(1)–C(31)	100.76(12)
C(2)–Mo–C(4)	171.07(10)	C(41)–P(2)–C(51)	102.90(11)
C(3)–Mo–C(4)	83.45(12)	C(41)–P(2)–C(61)	102.19(11)
C(2)–Mo–N	95.22(10)	C(51)–P(2)–C(61)	102.16(12)
C(3)–Mo–N	176.55(10)	C(1)–N–C(12)	115.5(2)
C(4)–Mo–N	93.64(11)	N–C(1)–C(42)	127.5(3)
C(11)–P(1)–Mo	100.74(9)	C(16)–C(11)–P(1)	125.6(2)
C(21)–P(1)–Mo	123.05(8)	C(12)–C(11)–P(1)	114.8(2)
C(31)–P(1)–Mo	120.59(9)	C(13)–C(12)–N	121.4(3)
C(41)–P(2)–Mo	106.77(8)	C(11)–C(12)–N	118.3(2)

to the P atoms. However these two W–C bonds (W–C(4) and W–C(5)) at 1.977(6) and 1.970(6) Å are both shorter than the two related *trans* distances of 2.035(6) and 2.016(6) Å for W–C(2) and W–C(3) respectively, a result not unexpected when the π acidity of the CO group is taken into account. The long distance between W and N (3.530(4) Å) indicates the absence of a bond between these two atoms. Support for the distinction made between the C and N atoms of the imine bridge on the basis of their thermal parameters comes from steric arguments. If these two atoms were interchanged then the H associated with the C would approach too closely to one of the carbonyl ligands (see Fig. 3).

Crystal structure of *cis*-[Cr(CO)$_4$(PNCHP-κ^2*P*,*N*)]·0.5CHCl$_3$ 5. In complex **5** (Fig. 4 and Table 6) there are two independent molecules in the asymmetric unit showing no significant differences from one another. One of the independent molecules (molecule A) has arbitrarily been selected for the purpose of this discussion. Complex **5** shows a much smaller deviation from the ideal octahedral co-ordination geometry than do **2** and **7** discussed previously. The N and one of the P atoms

Table 5 Selected bond lengths [Å] and angles [°] for *cis*-[$W(CO)_4$-(PNCHP-κ^2P,P')]·0.5$CHCl_3$

W–P(1)	2.5749(12)	P(2)–C(51)	1.833(5)
W–P(2)	2.5576(14)	P(2)–C(61)	1.845(5)
W–C(2)	2.035(6)	O(2)–C(2)	1.139(5)
W–C(3)	2.016(6)	O(3)–C(3)	1.150(5)
W–C(4)	1.977(6)	O(4)–C(4)	1.160(5)
W–C(5)	1.970(6)	O(5)–C(5)	1.156(6)
P(1)–C(11)	1.835(5)	N–C(1)	1.257(6)
P(1)–C(21)	1.841(5)	N–C(12)	1.405(6)
P(1)–C(31)	1.825(5)	C(1)–C(42)	1.451(6)
P(2)–C(41)	1.850(5)		
P(1)–W–P(2)	102.27(4)	C(5)–W–N	136.8(2)
P(1)–W–C(2)	82.84(13)	C(11)–P(1)–W	123.5(2)
P(1)–W–C(3)	94.93(13)	C(21)–P(1)–W	109.9(2)
P(1)–W–C(4)	168.3(2)	C(31)–P(1)–W	115.7(2)
P(1)–W–C(5)	86.7(2)	C(11)–P(1)–C(21)	102.5(2)
P(2)–W–C(2)	87.21(14)	C(11)–P(1)–C(31)	100.9(2)
P(2)–W–C(3)	90.93(14)	C(21)–P(1)–C(31)	101.5(2)
P(2)–W–C(4)	86.5(2)	C(41)–P(2)–C(51)	107.1(2)
P(2)–W–C(5)	171.0(2)	C(41)–P(2)–C(61)	101.8(2)
P(1)–W–N	55.25(7)	C(51)–P(2)–C(61)	96.5(2)
P(2)–W–N	51.08(7)	C(41)–P(2)–W	110.3(2)
C(2)–W–C(3)	176.7(2)	C(51)–P(2)–W	122.5(2)
C(2)–W–C(4)	90.0(2)	C(61)–P(2)–W	116.0(2)
C(2)–W–C(5)	93.3(2)	O(2)–C(2)–W	177.8(4)
C(3)–W–C(4)	92.6(2)	O(3)–C(3)–W	178.3(4)
C(3)–W–C(5)	89.0(2)	O(4)–C(4)–W	175.5(5)
C(4)–W–C(5)	84.5(2)	O(5)–C(5)–W	174.9(5)
C(2)–W–N	65.1(2)	C(1)–N–W	122.0(3)
C(3)–W–N	111.7(2)	C(12)–N–W	110.2(3)
C(4)–W–N	129.3(2)	C(1)–N–C(12)	125.6(4)

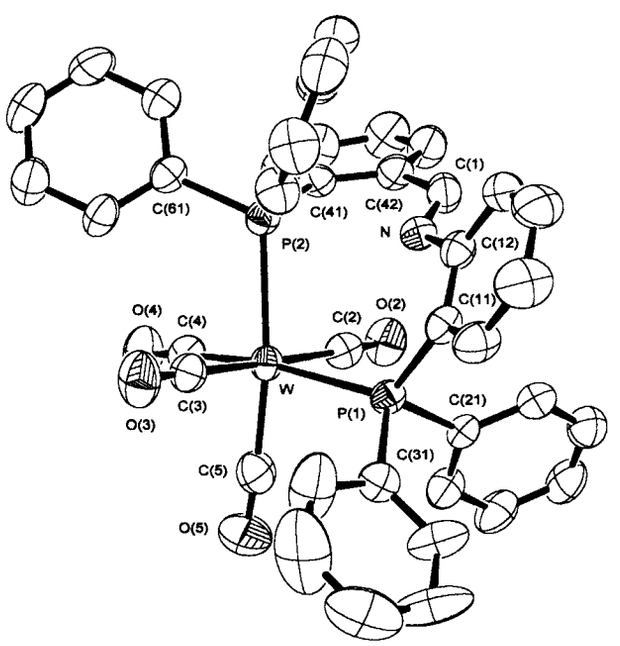

Fig. 3 An ORTEP diagram for the complex *cis*-[$W(CO)_4$(PNCHP-κ^2P,P')] **7**. Details as in Fig. 2.

occupy *cis* co-ordination sites forming a six-membered ring with a P(2A)–Cr(1)–N(1A) angle of 82.06(13)°.‡ As expected the carbonyl *trans* to the N atom (Cr(1)–C(4A)) has the shorter Cr–C distance of 1.794(7) Å than the carbonyl group *trans* to the P atom (Cr(1)–C(5A), 1.854(7) Å). The bond lengths and angles

‡ Previous studies (ref. 15) have indicated that PNCHP more readily binds a sulfur atom to the phosphorus atom three bonds removed from the imine nitrogen, implying that this maybe the more basic site. Incorporation of this P atom into the chelate ring in *cis*-[$Cr(CO)_4$(PNCHP)] would result in a five-membered ring. The single crystal structure shows that a six-membered ring is formed with the P atom four bonds removed from the co-ordinated imine N.

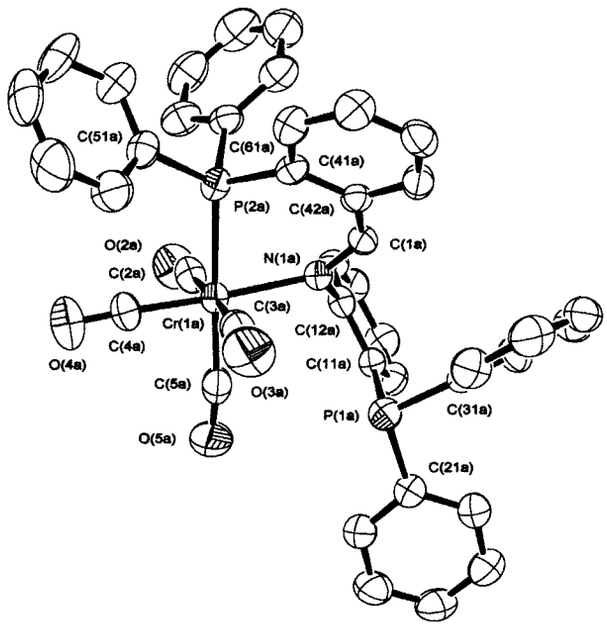

Fig. 4 An ORTEP diagram for the complex *cis*-[$Cr(CO)_4$(PNCHP-κ^2P,N)] **5**. Details as in Fig. 2.

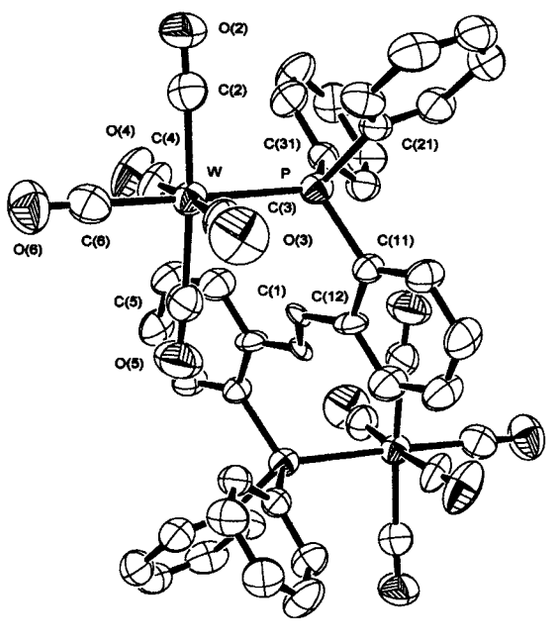

Fig. 5 An ORTEP diagram for the complex [{$W(CO)_5$}$_2$(PNCHP-κ^2P,P')] **9**. Details as in Fig. 2.

around the Cr are virtually identical to those of the related complex *cis*-[{$Cr(CO)_4$}$_2$(P_2N_2-κ^4P,N,N',P')], where P_2N_2 is *N*,*N*′-bis[*o*-(diphenylphosphino)benzylidene]ethylenediamine.[16]

Crystal structure of [{$W(CO)_5$}$_2$(PNCHP-κ^2P,P')]·2C_6H_5Me 9. The dinuclear complex **9** (Fig. 5 and Table 7), where two W atoms are linked by the PNCHP bridge, also shows a much smaller deviation from the ideal octahedral co-ordination geometry than do **2** and **7**. The W–P bond length of 2.554(2) Å is in accord with its counterparts in complex **7** and [$W(CO)_5$-(PCHO-κ^1P)] (PCHO = 2-diphenylphosphinobenzaldehyde) (2.561(1) Å[17]) and it is in a *trans* position to the shortest of the 5 W–C bonds. The C and N of the imine bridge were not distinguished due to the presence of the centre of symmetry at the midpoint of the C–N bond.

Electronic and infrared spectroscopy

The colour of the complex was a reliable visual aid for

Table 6 Selected bond lengths [Å] and angles [°] for *cis*-[Cr(CO)$_4$(PNCHP-κ^2*P*,*N*)] (Molecule A)

Cr(1)–P(2A)	2.3570(18)	P(2A)–C(51A)	1.825(6)
Cr(1)–N(1A)	2.141(5)	P(2A)–C(61A)	1.818(6)
Cr(1)–C(2A)	1.895(8)	O(2A)–C(2A)	1.141(7)
Cr(1)–C(3A)	1.879(8)	O(3A)–C(3A)	1.157(7)
Cr(1)–C(4A)	1.794(7)	O(4A)–C(4A)	1.162(6)
Cr(1)–C(5A)	1.854(7)	O(5A)–C(5A)	1.150(7)
P(1A)–C(11A)	1.830(6)	N(1A)–C(1A)	1.279(6)
P(1A)–C(21A)	1.828(6)	N(1A)–C(12A)	1.449(7)
P(1A)–C(31A)	1.825(6)	C(1A)–C(42A)	1.464(8)
P(2A)–C(41A)	1.817(6)		
N(1A)–Cr(1)–P(2A)	82.06(13)	C(21A)–P(1A)–C(31A)	105.6(3)
P(2A)–Cr(1)–C(2A)	95.0(2)	C(41A)–P(2A)–C(51A)	102.8(3)
P(2A)–Cr(1)–C(3A)	89.1(2)	C(41A)–P(2A)–C(61A)	102.1(3)
P(2A)–Cr(1)–C(4A)	94.3(2)	C(51A)–P(2A)–C(61A)	102.7(3)
P(2A)–Cr(1)–C(5A)	177.2(2)	C(41A)–P(2A)–Cr(1)	108.89(19)
C(2A)–Cr(1)–C(3A)	175.5(3)	C(51A)–P(2A)–Cr(1)	120.1(2)
C(2A)–Cr(1)–C(4A)	89.2(3)	C(61A)–P(2A)–Cr(1)	117.8(2)
C(2A)–Cr(1)–C(5A)	87.5(3)	O(2A)–C(2A)–Cr(1)	174.8(6)
C(3A)–Cr(1)–C(4A)	88.8(3)	O(3A)–C(3A)–Cr(1)	175.6(6)
C(3A)–Cr(1)–C(5A)	88.4(3)	O(4A)–C(4A)–Cr(1)	177.3(6)
C(4A)–Cr(1)–C(5A)	86.9(3)	O(5A)–C(5A)–Cr(1)	173.1(6)
C(2A)–Cr(1)–N(1A)	91.4(2)	C(1A)–N(1A)–Cr(1)	130.5(4)
C(3A)–Cr(1)–N(1A)	90.9(2)	C(12A)–N(1A)–Cr(1)	115.9(3)
C(4A)–Cr(1)–N(1A)	176.4(2)	C(1A)–N(1A)–C(12A)	113.6(5)
C(5A)–Cr(1)–N(1A)	96.7(2)	N(1A)–C(1A)–C(42A)	129.4(5)
C(11A)–P(1A)–C(21A)	100.3(3)	C(11A)–C(12A)–N(1A)	121.4(5)
C(11A)–P(1A)–C(31A)	100.2(3)	C(13A)–C(12A)–N(1A)	117.7(5)

Table 7 Selected bond lengths [Å] and angles [°] for [{W(CO)$_5$}$_2$-(PNCHP-κ^2*P*,*P*′)]·2C$_6$H$_5$Me

W–P	2.554(2)	P–C(31)	1.836(8)
W–C(2)	2.025(10)	O(2)–C(2)	1.152(9)
W–C(3)	1.998(10)	O(3)–C(3)	1.162(9)
W–C(4)	1.986(10)	O(4)–C(4)	1.162(9)
W–C(5)	2.036(10)	O(5)–C(5)	1.135(9)
W–C(6)	1.970(11)	O(6)–C(6)	1.167(10)
P–C(11)	1.838(7)	C(1)–C(1)#1	1.281(12)
P–C(21)	1.840(8)	C(1)–C(12)	1.427(10)
C(2)–W–P	89.7(2)	O(5)–C(5)–W	176.5(8)
C(3)–W–P	91.1(2)	O(6)–C(6)–W	179.0(8)
C(4)–W–P	92.1(2)	C(11)–P–W	115.5(2)
C(5)–W–P	93.4(2)	C(21)–P–W	116.3(3)
C(6)–W–P	178.2(2)	C(31)–P–W	115.0(3)
C(2)–W–C(3)	93.1(3)	C(11)–P–C(21)	101.1(3)
C(2)–W–C(4)	89.6(3)	C(11)–P–C(31)	106.5(3)
C(2)–W–C(5)	175.6(4)	C(21)–P–C(31)	100.6(3)
C(2)–W–C(6)	88.7(3)	C(12)–C(11)–P	120.9(6)
C(3)–W–C(4)	175.9(4)	C(16)–C(11)–P	119.9(6)
C(3)–W–C(5)	89.9(4)	C(22)–C(21)–P	122.0(6)
C(3)–W–C(6)	88.2(4)	C(26)–C(21)–P	118.6(6)
C(4)–W–C(5)	87.3(4)	C(32)–C(31)–P	124.1(6)
C(4)–W–C(6)	88.7(3)	C(36)–C(31)–P	117.5(6)
C(5)–W–C(6)	88.2(3)	C(1)#1–C(1)–C(12)	118.3(8)
O(2)–C(2)–W	177.1(8)	C(13)–C(12)–C(1)	121.7(7)
O(3)–C(3)–W	176.5(8)	C(11)–C(12)–C(1)	120.0(6)
O(4)–C(4)–W	177.1(7)		

Symmetry transformation used to generate equivalent atoms: #1 $-x,-y,-z$.

determining the environment of the imine nitrogen. In species where the nitrogen atom was co-ordinated an electronic absorption in the range 396 to 628 nm with ε_{max} values 1800 to 2700 L mol^{-1} cm^{-1} was observed as listed in Table 2. Metal-to-ligand charge transfer bands (MLCT) are expected when the ligand has low lying empty orbitals. Unsaturated ligands with empty π* orbitals are prime candidates.[18] Hence the absorption responsible for giving the complexes their characteristic 'rich' and intense colours as found for the blood red *cis*-[Cr(CO)$_4$-(PNCHP-κ^2*P*,*N*)] **5**, the crimson *fac*-[Mo(CO)$_3$(PNCHP-κ^3*P*,*N*,*P*′)] **4** and the dark blue, dark purple, and dark green of the *mer*-[M(CO)$_3$(PNCHP-κ^3*P*,*N*,*P*′)] **1**, **2**, **3** complexes is most likely a M ⟶ π*$_{imine}$ charge transfer. In further support of the assignment, the absorption exhibited ε_{max} values and solvatochromism (see Table 2) typical of a MLCT band.[18] Conversely, when the nitrogen atom was not co-ordinated, light reddish orange and yellow colours were observed, as found for the tetracarbonyl complexes *cis*-[M(CO)$_4$(PNCHP-κ^2*P*,*P*′)] (M = Mo **6** or W **7**) and for all the pentacarbonyl complexes.

The contrasting colours of the light reddish orange molybdenum and tungsten tetracarbonyl complexes in comparison to the intense dark red of the chromium tetracarbonyl complex can now be explained in terms of the absence of the **M** ⟶ π*$_{imine}$ charge transfer band in the former cases. For molybdenum or tungsten complexes, both phosphorus atoms of PNCHP are co-ordinated with the nitrogen atom non-co-ordinated, as confirmed by ^{31}P NMR spectroscopy and X-ray crystallography. In contrast, the chromium tetracarbonyl complex has only one phosphorus atom bound, with the imino nitrogen atom binding in preference to the second phosphorus atom. This phenomenon can be explained by evoking the Hard Soft Acid Base (HSAB) principle. This co-ordination set is also observed in the 'P_2N_2' ligand *N*,*N*′-bis[*o*-(diphenylphosphino)-benzylidene]ethylenediamine which binds to the 'Cr(CO)$_4$' moiety *via* one of its two phosphorus donor atoms and one imine nitrogen atom.[16]

The wavenumbers and number of IR bands in the carbonyl stretching region (Table 2) are typical for each type of carbonyl species.[9,16,19–21] When the imine nitrogen was non-co-ordinated, as found for the pentacarbonyl and molybdenum and tungsten tetracarbonyl complexes, the ν(C=N) band was at similar or slightly higher wavenumbers when compared with the free PNCHP ligand (1620 cm^{-1}). However, as expected, when the imine nitrogen was co-ordinated, the ν(C=N) band was lowered by 35 to 50 cm^{-1} in energy as shown in Table 2.

NMR spectroscopy

Proton NMR spectra (Table 1) showed the expected integration and peak multiplicities. In all complexes where the phosphorus nearest to the imine carbon of PNCHP was involved in co-ordination, the imine proton signal shifts to lower frequencies relative to 'free' PNCHP [δ 8.92, ^4J(PH) 5.5 Hz] and the P–H coupling is no longer observed. In contrast, for the complexes where this phosphorus was non-co-ordinated a higher frequency shift was observed, as seen in the mixtures of the

$[M(CO)_5(PNCHP\text{-}\kappa^1P)]$ (M = Cr **10a**, **10b** or W **11a**, **11b**) complexes.

When one equivalent of PNCHP is treated with the '$M(CO)_5$' (M = Cr or W) moiety both phosphorus co-ordination isomers are obtained. However, the ratio of the two isomers is not a statistical 1 : 1 mixture but 2 : 1 in favour of **10a** and **11a**. This was concluded by considering the NMR signal multiplicity of the imine proton. In the "free" PNCHP ligand it is split by the phosphorus nucleus nearest to the imine carbon (^4J(PH) = 5.5 Hz). However, when the same phosphorus is bound to sulfur, as in PNCHP=S, the imine proton is a singlet suggesting that co-ordination of the phosphorus four bonds removed from the nitrogen means that P–H coupling is no longer observed. When sulfur is bound to the other phosphorus atom, as in S=PNCHP, a doublet imine proton is observed.[15] The complexes $[Cr(CO)_5(PNCHP\text{-}\kappa^1P)]$ **10a** and $[W(CO)_5(PNCHP\text{-}\kappa^1P)]$ **11a** both display doublet imine proton signals while $[Cr(CO)_5(PNCHP\text{-}\kappa^1P)]$ **10b** and $[W(CO)_5(PNCHP\text{-}\kappa^1P)]$ **11b** have singlet signals (Table 1). The comparable ligand *N*-(2-diphenylphosphinobenzylidene)-2-(2-pyridyl)ethylamine[22] shows no imine proton–phosphorus coupling in the "free" ligand, further supporting the imine proton coupling assignment in PNCHP. Hence we have assigned the major isomer of the above reaction to $[M(CO)_5(PNCHP\text{-}\kappa^1P)]$ **10a**, **11a** and the minor isomer to $[M(CO)_5(PNCHP\text{-}\kappa^1P)]$ **10b**, **11b** based on the chemical shifts and coupling constants listed in Table 1 and supported by the reaction of sulfur with PNCHP. These assignments have allowed us to assign the weakest resonances in the ^{31}P NMR spectra to the minor isomer **10b** and **11b**. ^1J(WP) coupling values of 244 and 242 Hz respectively are typical.[23]

The ^{31}P NMR data, shown in Table 1, of the molybdenum and tungsten tetracarbonyl species showed all phosphorus nuclei resonances at higher frequency than the 85% H_3PO_4 reference, with an AB splitting pattern and coupling constants of 26 and 27 Hz respectively. This is indicative of PNCHP co-ordinated through both phosphorus atoms in *cisoid* fashion.[24] In contrast, the chromium tetracarbonyl species showed only one phosphorus nuclei resonance at higher frequency than H_3PO_4, the other resonance being at a lower frequency with no phosphorus–phosphorus coupling. This is consistent with one co-ordinated and one non-co-ordinated P^{III} respectively. A small amount (<5%) of another chromium species with δ 55.4 and δ 38.4, ^2J(PP) 35 Hz, is observed in the ^{31}P NMR spectrum of the crude product. This is most likely the chromium analogue of the 'P,P'-bound molybdenum and tungsten complexes. The expected tungsten satellites are observed in the ^{31}P NMR spectrum of *cis*-$[W(CO)_4(PNCHP\text{-}\kappa^2P,P')]$ **7**, the ^1J(WP) values of 238 and 233 Hz being typical.[23,25]

The most significant differences found in the ^{31}P NMR spectra of the tricarbonyl complexes (compared to the tetracarbonyl species) are the much larger ^2J(PP) coupling constants of *ca.* 90 Hz. These are indicative of a *transoid* arrangement of the phosphorus atoms around the metal,[24] supporting a meridional arrangement of the PNCHP ligand. In general the tricarbonyl species exhibit shifts of some 20 ppm higher in frequency than their tetracarbonyl counterparts which is possibly due to the increased ring strain, particularly for the five membered ring component,[25] when PNCHP behaves as a tridentate ligand. The isomer *fac*-$[Mo(CO)_3(PNCHP\text{-}\kappa^3P,N,P')]$ **4** displays a ^2J(PP) coupling constant of 26 Hz typical of *cisoid* phosphorus atoms, hence supporting the *fac* isomer assignment.[26]

Kinetic and equilibrium studies

Preliminary studies of the geometrical isomerisation of *fac*-$[Mo(CO)_3(PNCHP\text{-}\kappa^3P,N,P')]$ **4** to *mer*-$[Mo(CO)_3(PNCHP\text{-}\kappa^3P,N,P')]$ **2** were made in acetone, acetonitrile, chloroform and dichloromethane by following the increase in the absorbance at 700 nm as the purple **2** product formed. The *fac*-to-*mer* isomerisation proceeds with considerable complex decomposition in chloroform and to a lesser, but still significant, extent in dichloromethane while solubility problems were encountered with acetonitrile as solvent at the lower temperatures. In acetone the solubility was sufficient and the isomerisation took place without decomposition over the temperature range 19.5–49.5 °C. Hence, comprehensive kinetic and thermodynamic parameters could only be obtained for the isomerisation in this solvent. As depicted in eqn. (1), k_1 and k_{-1} denote

$$fac \underset{k_{-1}}{\overset{k_1}{\rightleftharpoons}} mer \qquad (1)$$

the forward and reverse rate constants, respectively. There was no spectroscopic evidence for detectable concentrations of any intermediates. In each kinetic run, a plot of $\ln(A - A_\infty)$ *versus* time gave a straight line for at least three half-lives (A and A_∞ denote the absorbance at 700 nm at time t and at infinite time respectively, where the *fac–mer* mixture was at thermodynamic equilibrium). The slope gave the first-order rate constant k_{obsd} which was determined at four different temperatures (19.5, 29.7, 40.0 and 49.5 °C). The rate constants for isomerisation were calculated from the equilibrium constant K_{eq}, obtained from the integrated ^{1}H NMR signals of the imine proton in equilibrated solutions (eqn. 2), and the observed rate constant

$$K_{eq} = k_1/k_{-1} = \int \delta CH{=}N_{mer} / \int \delta CH{=}N_{fac} \qquad (2)$$

(eqn. 3). The K_{eq} value was found to be 7.3 and independent of

$$k_{obsd} = k_1 + k_{-1} \qquad (3)$$

temperature in acetone. The k_{obsd} values along with the forward (k_1) and reverse (k_{-1}) rate constants are collected in Table 3. The activation enthalpies for the forward ($\Delta H_1^{\ddagger}$) and reverse ($\Delta H_{-1}^{\ddagger}$) reactions were 95 ± 3 and 94 ± 2 kJ mol^{-1}, respectively. The activation entropies for the forward ($\Delta S_1^{\ddagger}$) and reverse ($\Delta S_{-1}^{\ddagger}$) reactions were −14.1 ± 0.7 and −36 ± 2 J K^{-1} mol^{-1}, respectively.

Driving forces for *fac–mer* isomerisation can be attributed to electronic advantages and/or steric pressure exerted by the ligands around the metal.[4,27] In this case the PNCHP ligand prefers to be coplanar, as it is in the *mer* isomer. This is probably due to the structural rigidity and inherent inflexibility of the PNCHP ligand imposed on the ligand by the imine double bond with the phosphino moieties locked *trans* to the double bond.

In general, a large positive activation enthalpy (>100 kJ mol^{-1}), that is of bond breaking magnitude, coupled with a positive activation entropy is supportive of a dissociative mechanism whilst a small activation enthalpy, less than bond breaking magnitude, coupled with a large negative entropy (≈−200 J K^{-1} mol^{-1}) is supportive of a twist mechanism.[28] For our system, $\Delta H_1^{\ddagger}$ and $\Delta H_{-1}^{\ddagger}$ values of 95 and 94 kJ mol^{-1} coupled respectively with $\Delta S_1^{\ddagger}$ and $\Delta S_{-1}^{\ddagger}$ values of −14.1 and −36 J K^{-1} mol^{-1} are inconclusive with respect to which mechanism the isomerisation follows. Note that if solvent restriction occurs $\Delta S^{\ddagger}$ could be negative for a dissociative mechanism. Rate constants did decrease slightly with increasing co-ordinating powers of the solvent. For example, for the co-ordinating solvent acetonitrile, the rate constant halves compared with acetone whilst moving to the poor co-ordinating solvent dichloromethane the rate constant doubles. One might equate this observation with a dissociative mechanism, however the addition of Et_3N to acetone did not affect the rate. In addition, whilst following the isomerisation by ^{31}P NMR in the presence of a tenfold excess of triphenyl phosphite no intermediates on the NMR timescale were detected. Triphenyl phosphite may have been expected to bind to the metal if a dissociative mechanism was in effect. Without thermodynamic activation parameters for the isomerisation in

acetonitrile and dichloromethane, a more substantial conclusion with respect to the solvent effect cannot be drawn.

Conclusion

Related compounds of the type [{M(CO)$_x$}$_y$(PNCHP)] where M is Cr, Mo or W and $x = 3$, 4 or 5, and $y = 1$ or 2 have been synthesized. The 'P$_2$N' mixed donor multidentate ligand PNCHP adopts κ^2*P*,*N cis* co-ordination in *cis*-[Cr(CO)$_4$(PNCHP-κ^2*P*,*N*)] but a κ^2*P*,*P′ cis* co-ordination for the complexes of Mo and W. For the compounds [M(CO)$_3$(PNCHP-κ^3*P*,*N*,*P′*)], PNCHP co-ordinates in a *mer* fashion. The *fac* isomer is also isolatable for Mo but readily converts into the *mer* isomer. The first-order forward rate constants (k_1) for the *fac*-to-*mer* isomerism in acetone are 1.22×10^{-5}, 4.18×10^{-5}, 1.72×10^{-4} and 4.89×10^{-4} s^{-1} at 19.5, 29.7, 40.0 and 49.5 °C respectively, with thermodynamic activation parameters $\Delta H_1^{\ddagger}$ and $\Delta S_1^{\ddagger}$ of 95 kJ mol^{-1} and −14.1 J K^{-1} mol^{-1} respectively. For [M(CO)$_5$(PNCHP-κ^1*P*)] (M = Cr or W) the favoured binding mode is *via* the phosphorus atom nearest to the imine nitrogen atom. PNCHP will also bridge (*via* the two phosphorus atoms) two pentacarbonyl moieties.

Experimental

Materials and instrumentation

NMR measurements were performed on a JEOL GX270W spectrometer. IR spectra were recorded on a BIO-RAD FTS-40 instrument, UV-vis spectra using a Shimadzu UV-310PC UV-VIS-NIR scanning spectrometer. Mass spectra were obtained using a Varian VG70-250S double-focussing magnetic sector spectrometer by the method of liquid ion secondary mass spectroscopy (LSIMS) using *m*-nitrobenzyl alcohol as the matrix. Isotope abundance calculations were performed to identify the parent ion. Microanalyses were performed by the Campbell Microanalytical Laboratory, University of Otago. 2-Diphenylphosphinobenzaldehyde (2-PCHO),[29] 2-aminophenyldiphenylphosphine (2-PNH$_2$),[30] [Cr(CO)$_4$(NBD)],[31] [M(CO)$_4$(pip)$_2$] (pip = piperidine) (M = Mo or W)[32] and [Mo(CO)$_3$(CHT)][33] (CHT = cycloheptatriene) were prepared according to literature. Solvents were dried by standard procedures. All reactions were carried out under an inert atmosphere.

Syntheses

2-(Diphenylphosphino)-*N*-[(2-diphenylphosphino)benzylidene]-aniline (PNCHP). To a three-necked flask fitted with a Dean-Stark trap and condenser was added 2-PCHO (1.160 g, 4 mmol), 2-PNH$_2$ (1.108 g, 4 mmol), toluene-*p*-sulfonic acid (20 mg, 0.10 mmol) and benzene (120 cm^3). The solution was refluxed for 7 h and then the solvent removed by rotary evaporation to produce a yellow oil. This was dissolved in the minimum amount of dichloromethane, then methanol was added until crystallisation began. After standing for half an hour PNCHP was filtered off as pale yellow crystals, washed with methanol and dried *in vacuo.* A second crop was obtained by concentration of the mother liquor by rotary evaporation and crystallisation from dichloromethane–methanol. Yield: 1.825 g (80%). mp 176–178°C. IR: 1620 cm^{-1} [*ν*(C=N)].

***mer*-[Cr(CO)$_3$(PNCHP-κ^3*P*,*N*,*P′*)]·2C$_6$H$_5$Me 1.** A mixture of [Cr(CO)$_4$(NBD)] (0.143 g, 0.558 mmol) and PNCHP (0.306 g, 0.557 mmol) in 25 mL of toluene was heated to reflux for 1.5 h giving a dark green solution. The cooled solution was filtered through Kieselguhr and the filtrate allowed to stand overnight. The resulting solid was isolated, washed with n-pentane and dried *in vacuo*, yielding 0.130 g (34%) of *mer*-[Cr(CO)$_3$(PNCHP-κ^3*P*,*N*,*P′*)]·2C$_6$H$_5$Me as dark green crystals, mp 207–210 °C.

***mer*-[Mo(CO)$_3$(PNCHP-κ^3*P*,*N*,*P′*)]·CH$_2$Cl$_2$ 2.** A mixture of [Mo(CO)$_3$(CHT)] (0.140 g, 0.529 mmol) and PNCHP (0.291 g, 0.530 mmol) in 25 mL of toluene was heated to reflux for 25 min giving a dark blue solution. The cooled solution was filtered through Kieselguhr and the filtrate allowed to stand overnight. The resulting solid was isolated, washed with n-pentane and dried *in vacuo,* to give *mer*-[Mo(CO)$_3$(PNCHP-κ^3*P*,*N*,*P′*)]·CH$_2$Cl$_2$ as dark blue crystals, mp 114–115 °C.

***fac*-[Mo(CO)$_3$(PNCHP-κ^3*P*,*N*,*P′*)] 4.** An ice-cold solution of [Mo(CO)$_3$(CHT)] (0.099 g, 0.365 mmol) dissolved in toluene was added to an ice-cold solution of PNCHP (0.200 g, 0.364 mmol) dissolved in toluene. The mixture was stirred for *ca*. 1 h, keeping the temperature below 0 °C, followed by 23 h at room temperature. The resulting precipitate was isolated, washed with n-pentane, and dried *in vacuo*, yielding 0.215 g (73%) of *fac*-[Mo(CO)$_3$(PNCHP-κ^3*P*,*N*,*P′*)] as a crimson powder, mp 154–155 °C.

***mer*-[W(CO)$_3$(PNCHP-κ^3*P*,*N*,*P′*)]·CH$_2$Cl$_2$ 3.** A mixture of *cis*-[W(CO)$_4$(pip)$_2$] (0.206 g, 0.440 mmol) and PNCHP (0.243 g, 0.440 mmol) in 10 mL of toluene was heated to reflux for 2.5 h giving a dark blue solution. The solvent volume was reduced *in vacuo* to approximately 5 mL and the solution allowed to stand overnight to give dark purple crystals. The crystals were isolated then recrystallised from dichloromethane–methanol at 5 °C yielding 0.129 g (36%) of *mer*-[W(CO)$_3$(PNCHP-κ^3*P*,*N*,*P′*)]·CH$_2$Cl$_2$ as a dark purple crystalline solid, mp 118–123 °C.

***cis*-[Cr(CO)$_4$(PNCHP-κ^2*P*,*N*)] 5.** A mixture of [Cr(CO)$_4$(NBD)] (0.039 g, 0.151 mmol) and PNCHP (0.083 g, 0.151 mmol) in 12 mL of dichloromethane–acetonitrile (1 : 1) was stirred at room temperature for 48 h. The resulting dark brownish red precipitate of *cis*-[Cr(CO)$_4$(PNCHP-κ^2*P*,*N*)] was isolated by filtration, washed with n-pentane and dried *in vacuo*. The filtrate was allowed to stand for two days, under argon, giving a second crop of dark brownish-red microcrystals. The combined yield was 0.077 g (71%), mp 196–200 °C (decomp.).

***cis*-[Mo(CO)$_4$(PNCHP-κ^2*P*,*P′*)] 6.** A mixture of *cis*-[Mo(CO)$_4$(pip)$_2$] (0.201 g, 0.531 mmol) and PNCHP (0.294 g, 0.534 mmol) in 10 mL of dichloromethane was heated to reflux for 15 min. The dark red solution was filtered through Kieselguhr and the solvent volume reduced *in vacuo* to approximately 3 mL. Co-crystallisation of reddish orange and maroon crystals occurred on the addition of *ca*. 1–2 mL of methanol after 3 h at 5 °C. Both crystal types were isolated, washed with cold methanol and dried *in vacuo*, to give a combined yield of 0.364 g (90%). Separation of the two products was achieved by washing away the very soluble maroon product with chloroform, leaving behind the less soluble *cis*-[Mo(CO)$_4$(PNCHP-κ^2*P*,*P′*)] as reddish orange crystals, mp 168–170 °C (decomp.).

***cis*-[W(CO)$_4$(PNCHP-κ^2*P*,*P′*)] 7.** A mixture of *cis*-[W(CO)$_4$(pip)$_2$] (0.201 g, 0.431 mmol) and PNCHP (0.238 g, 0.435 mmol) in 10 mL of toluene was heated to *ca.* 60 °C until all of the *cis*-[W(CO)$_4$(C$_5$H$_{11}$N)$_2$] had been taken up into solution (*ca.* 30 min). The resulting clear green solution was allowed to cool and then filtered through Kieselguhr. Crystallisation was initiated by solvent volume reduction *in vacuo.* The mixture was then kept at 5 °C for 3–4 h. The reddish orange solid that formed was isolated by filtration and washed with toluene then recrystallised from dichloromethane to yield 0.091 g (25%) of *cis*-[W(CO)$_4$(PNCHP-κ^2*P*,*P′*)] as a red crystalline solid, mp 187–190 °C (decomp.).

The reaction of Cr(CO)$_6$ with PNCHP to give complexes 10a and 10b. [Cr(CO)$_6$] (0.223 g, 1.01 mmol) in 30 mL of tetra-

hydrofuran was irradiated using a UV lamp for 1 h, resulting in an orange solution. PNCHP (0.538 g, 0.979 mmol) in 15 mL of tetrahydrofuran was added and the red solution stirred for 30 min. The solution was filtered through Kieselguhr. The solvent was removed and unchanged $[Cr(CO)_6]$ sublimed, *in vacuo*. Preparative scale, thin layer chromatography, eluting with dichloromethane–n-hexane (1:1), was used to isolate a $[Cr(CO)_5(PNCHP\text{-}\kappa^1P)]$–$[Cr(CO)_5(PCHNP\text{-}\kappa^1P)]$ **10a**–**10b** mixture (2:1), however, these two isomers could not be separated. In addition, the mixture could not be isolated as an analytically pure solid since conversion into tetracarbonyl species occurred.

The reaction of $W(CO)_6$ with PNCHP to give complexes 11a and 11b. $[W(CO)_6]$ (0.130 g, 0.367 mmol) in 30 mL of tetrahydrofuran was irradiated for 1 h, resulting in a yellow solution. PNCHP (0.222 g, 0.409 mmol) in 20 mL of tetrahydrofuran was added and the orange solution stirred for 40 min. The solvent and any unchanged $[W(CO)_6]$ were removed *in vacuo*. The resulting orange-red oil was dissolved in hot dichloromethane under a stream of argon gas, then cooled to 5 °C. After 48 h a mixture of $[W(CO)_5(PNCHP\text{-}\kappa^1P)]$ **11a** and $[W(CO)_5(PCHNP\text{-}\kappa^1P)]$ **11b** (2:1) was isolated as a pale yellow solid.

$[\{Cr(CO)_5\}_2(PNCHP\text{-}\kappa^2P,P')]$ 8. $[Cr(CO)_6]$ (0.201 g, 0.913 mmol) in 25 mL of tetrahydrofuran was irradiated for 1 h, resulting in an orange solution. PNCHP (0.250 g, 0.455 mmol) in 15 mL of tetrahydrofuran was added and the now orange solution stirred for 30 min. The solvent and any unchanged $[Cr(CO)_6]$ were removed *in vacuo*. The resulting residue was dissolved in toluene and filtered to remove insoluble solids. The filtrate was allowed to stand for 48 h at 5 °C under argon. $[\{Cr(CO)_5\}_2(PNCHP\text{-}\kappa^2P,P')]$ was isolated as yellow crystals, washed with n-pentane and dried *in vacuo* to yield 0.166 g (39%), mp 160 °C (decomp.).

$[\{W(CO)_5\}_2(PNCHP\text{-}\kappa^2P,P')]$ 9. $[W(CO)_6]$ (0.400 g, 1.14 mmol) in 25 mL of tetrahydrofuran was irradiated for 1 h, resulting in a yellow solution. PNCHP (0.312 g, 0.568 mmol) in 15 mL of tetrahydrofuran was added and the orange solution stirred for 45 min. The solvent and any unchanged $[W(CO)_6]$ were removed *in vacuo*. The resulting residue was dissolved in toluene and filtered to isolate insoluble tan solids. These were dissolved in boiling toluene, under a stream of argon gas, and the resulting solution allowed to stand for 48 h at 5 °C. $[\{W(CO)_5\}_2(PNCHP\text{-}\kappa^2P,P')]$ was isolated as yellow diamond shaped crystals, washed with n-pentane and dried *in vacuo* to give 0.320 g (47%), mp 241–246 °C.

Crystallography

Crystal data. *Complex* ***2****, mer-[Mo(CO)$_3$(PNCHP-κ^3P,N,P′)]·2C$_6$H$_5$Me.* $C_{54}H_{45}MoNO_3P_2$, $M = 913.79$, monoclinic, $a = 12.490(10)$, $b = 17.680(10)$, $c = 20.630(10)$ Å, $\beta = 90.76(3)°$, $U = 4555(5)$ Å^3, $T = 292$ K, space group $P2_1/c$, $Z = 4$, μ(Mo-Kα) = 0.40 mm^{-1}, 8394 reflections measured, 8000 unique ($R_{int} = 0.0160$) which were used in all calculations. The final $Rw(F_o^2) = 0.0801$, $R(F_o) = 0.0416$.

Complex ***5****, cis-[Cr(CO)$_4$(PNCHP-κ^2P,N)].* $C_{41}H_{29}CrNO_4P_2$, $M = 713.59$, monoclinic, $a = 14.429(3)$, $b = 29.433(6)$, $c = 17.389(3)$ Å, $\beta = 108.40(3)°$, $U = 7007(2)$ Å^3, $T = 295$ K, space group $P2_1/c$, $Z = 8$, μ(Mo-Kα) = 0.461 mm^{-1}, 6871 reflections measured, 6533 unique ($R_{int} = 0.0359$) which were used in all calculations. The final $Rw(F_o^2) = 0.1030$, $R(F_o) = 0.0363$.

Complex ***7****, cis-[W(CO)$_4$(PNCHP-κ^2P,P′)]·0.5CHCl$_3$.* $C_{41.5}H_{29.5}Cl_{1.5}NO_4P_2W$, $M = 904.62$, monoclinic, $a = 23.476(5)$, $b = 18.128(4)$, $c = 19.254(4)$ Å, $\beta = 116.08(3)°$, $U = 7360(3)$ Å^3, space group $C2/c$, $Z = 8$, μ(Mo-Kα) = 3.38 mm^{-1}, 7068 reflections measured, 3438 unique ($R_{int} = 0.0198$) which were used in all calculations. The final $Rw(F_o^2) = 0.0450$, $R(F_o) = 0.0281$.

Complex ***9****, [{W(CO)$_5$}$_2$(PNCHP-κ^2P,P′)]·2C$_6$H$_5$Me.* $C_{61}H_{44}NO_{10}P_2W_2$, $M = 1378.61$, triclinic, $a = 10.387(2)$, $b = 12.076(2)$, $c = 12.229$ Å, $\alpha = 98.79(3)$, $\beta = 100.59(3)$, $\gamma = 107.99(3)°$, $U = 1397.6(4)$ Å^3, $T = 290$ K, space group $P\bar{1}$, $Z = 1$, μ(Mo-Kα) = 4.23 mm^{-1}, 2754 reflections measured, 2588 unique ($R_{int} = 0.0271$) which were used in all calculations. The final $Rw(F_o^2) = 0.0653$, $R(F_o) = 0.0384$.

X-Ray analysis. Single crystals of the complexes were grown as described under their respective syntheses and attached to the ends of glass fibres with cyanoacrylate glue. Data collection, solution and refinement were performed as previously described.[34–36] Solvent molecules were located in **2**, **7** and **9**. In complex **2** two molecules of toluene were found, the first of which appeared to show little signs of disorder. However the second was disordered over two sites with occupancy factors of 0.579 and 0.421 and the atoms of each ring were refined as a rigid group. In **7** a half-weighted chloroform molecule was located. The half-weighted nature results from the close approach (C(81)–C(81′) 0.87 Å) of a symmetry-related chloroform molecule in the unit cell. Isotropic thermal motion was assumed for C(81) of this group. In **9** the complex lies across a centre of symmetry with the centre at the midpoint of the C–N bond. No attempt was made to distinguish the C and N atoms by assigning the space group as *P*1 and they were included in the calculations as C. The molecule of toluene located in the asymmetric unit showed little signs of disorder. No solvent was located in **5**.

CCDC reference number 186/2053.

See http://www.rsc.org/suppdata/dt/b0/b002427i/ for crystallographic files in .cif format.

Kinetic and equilibrium studies of complex 4

Acetone was freshly distilled over 4A molecular sieves, chlorinated solvents and acetonitrile were freshly distilled over CaH_2 and all were degassed with argon. Stock solutions of *fac*-$[Mo(CO)_3(PNCHP\text{-}\kappa^3P,N,P')]$ **4** were prepared by dissolving an appropriate amount of the solid complex immediately before each experiment. Samples were transferred to a 1 cm path-length sealed quartz cuvette placed in the constant temperature (±3%) jacket of the spectrometer. Kinetic runs as a function of temperature (19.5–49.5 °C) were performed with a HP 8452A uv-vis spectrometer at 700 nm. Absorbance readings were taken until the reaction had progressed to equilibrium. Values of k_{obsd} were obtained from linear plots of $\ln(A - A_\infty)$ against time, using a minimum of 6 absorbance/time pairs. The first-order rate constants were calculated using a linear regression method. All plots gave correlation coefficients greater than 0.9993. Activation energy was calculated from an Arrhenius plot and activation enthalpy and entropy from an Eyring plot.

Acknowledgements

We thank the Massey University Research Fund for financial support.

References

1 See for example, G. Franciò, R. Scopelliti, C. G. Arena, G. Bruno, D. Drommi and F. Faraone, *Organometallics*, 1998, **17**, 338; R. Noyori and S. Hashiguchi, *Acc. Chem. Res.*, 1997, **30**, 97; F. Ungváry, *Coord. Chem. Rev.*, 1997, **167**, 233; A. Carmona, A. Corma, M. Iglesias, A. San José and F. Sánchez, *J. Organomet. Chem.*, 1995, **492**, 11.
2 C. Bianchini, J. A. Casares, M. Peruzzini, A. Romerosa and F. Zanobini, *J. Am. Chem. Soc.*, 1998, **118**, 4585.
3 J. Kleverlaan, F. Hartl and D. J. Stufkens, *J. Organomet. Chem.*, 1998, **561**, 57.
4 S. C. N. Hsu and W.-Y. Yeh, *J. Chem. Soc.*, *Dalton Trans.*, 1998, 125 and refs. therein.
5 A. Rodger and B. F. G. Johnson, *Inorg. Chem.*, 1998, **27**, 3062.

6 J. A. S. Howell, P. C. Yates, N. F. Ashford, D. T. Dixon and R. Warren, *J. Chem. Soc.*, *Dalton Trans.*, 1996, 3959.
7 R. G. Wilkins, *Kinetics and Mechanism of Reactions of Transition Metal Complexes*, 2nd edn., VCH, Weinheim, 1991.
8 R. G. Compton, J. C. Eklund, A. Hallik, S. Kumbhat, A. M. Bond and R. Colton, *J. Chem. Soc.*, *Perkin Trans. 2*, 1995, 1327.
9 A. Jacobi, G. Huttner and U. Winterhalter, *Chem. Ber./Recueil*, 1997, **130**, 1279.
10 C. K. Johnson, ORTEP II, Report ORNL-5138, Oak Ridge National Laboratory, Oak Ridge, TN, 1976.
11 D.-N Horng and C.-H. Ueng, *Inorg. Chim. Acta*, 1995, **232**, 175.
12 F. A. Cotton, D. J. Darensbourg, S. Klein and B. W. S. Kolthammer, *Inorg. Chem.*, 1982, **21**, 294.
13 *International Tables for X-Ray Crystallography*, Kynoch Press, Birmingham, 1962, vol. III.
14 See for example, T. E. Burrow, D. L. Hughes, A. J. Lough, M. J. Maguire, R. H. Morris and R. L. Richards, *J. Chem. Soc.*, *Dalton Trans.*, 1995, 1315.
15 E. W. Ainscough, A. M. Brodie, A. K. Burrell, X. Fan, M. J. R. Halstead, S. M. F. Kennedy and J. M. Waters, *Polyhedron*, submitted for publication.
16 W. Wong, J. Gao, Z. Zhou and T. Mak, *Polyhedron*, 1992, **11**, 2965.
17 E. W. Ainscough, A. M. Brodie, S. L. Ingham and J. M. Waters, *Inorg. Chim. Acta*, 1995, **234**, 163.
18 A. B. P. Lever, *Inorganic Electronic Spectroscopy*, 2nd edn., Elsevier, Amsterdam, 1984.
19 S. O. Grim, W. L. Briggs, R. C. Barth, C. A. Tolman and J. P. Jesson, *Inorg. Chem.*, 1974, **13**, 1095.
20 U. U. Ike, S. D. Perera, B. L. Shaw and M. Thornton-Prett, *J. Chem. Soc.*, *Dalton Trans.*, 1995, 2057.
21 M. A. Paz-Sandoval, M. E. Domínguez-Durán, C. Pazos-Mayen, A. Ariza-Castolo, M. D. Rosales-Hoz and R. Contreras, *J. Organomet. Chem.*, 1995, **492**, 1.
22 P. Wehman, R. E. Rülke, V. E. Kaasjager, P. C. J. Kramer, H. Kooijman, A. L. Spek, C. J. Elsevier, K. Vrieze and P. W. N. M. van Leeuwen, *J. Chem. Soc.*, *Chem. Commun.*, 1995, 331.
23 J. W. Benson, E. A. Keiter and R. L. Keiter, *J. Organomet. Chem.*, 1995, **495**, 77.
24 J. Mason (Editor), *Multinuclear NMR*, Plenum Press, New York, 1987.
25 T. Lin, S. Sun, J. J. Wu, L. Lee, K. Lin and Y. F. Huang, *Inorg. Chem.*, 1995, **34**, 2323.
26 S. D. Perera, B. L. Shaw and M. Thornton-Prett, *J. Chem. Soc.*, *Dalton Trans.*, 1992, 1469.
27 M. Cano, J. A. Campo, V. Pérez-García, E. Gutiérrez-Puebla and C. Alvarez-Ibarra, *J. Organomet. Chem.*, 1990, **382**, 397.
28 A. A. Ismail, F. Sauriol and S. Butler, *Inorg. Chem.*, 1989, **28**, 1007.
29 M. K. Cooper, J. M. Downes and P. A. Duckworth, *Inorg. Synth.*, 1989, **25**, 129.
30 J. E. Hoots, T. B. Rauchfuss and D. A. Wrobleski, *Inorg. Synth.*, 1982, **21**, 175.
31 R. B. King, *Organometallic Synthesis*, Academic Press, 1965, vol. 1, p. 122.
32 D. J. Darensbourg and R. L. Kump, *Inorg. Chem.*, 1978, **17**, 2680.
33 F. A. Cotton, J. A. McCleverty and J. E. White, *Inorg. Synth.*, 1967, **9**, 121.
34 S. E. Page, K. C. Gordon and A. K. Burrell, *Inorg. Chem.*, 1998, **37**, 4452.
35 Computations were performed with the Structure Determination Package SDP, Enraf-Nonius, Delft, 1985.
36 G. M. Sheldrick, SHELXL 93. Institut für Anorganische Chemie der Universität Göttingen, 1993.